Appl. Phys. A 83, 329–332 (2006)
DOI: 10.1007/s00339-006-3498-z

Applied Physics A
Materials Science & Processing

Z.Y. ZHENG[1]
J. ZHANG[1,✉]
X. LU[1]
Z.Q. HAO[1]
X.H. YUAN[1,2]
Z.H. WANG[1]
Z.Y. WEI[1]

Characteristic investigation of ablative laser propulsion driven by nanosecond laser pulses

[1] Laboratory of Optical Physics, Institute of Physics, Chinese Academy of Sciences, Beijing 100080, P.R. China
[2] State Key Laboratory of Transient Optics Technology, Chinese Academy of Sciences, Xi'an 710068, P.R. China

Received: 24 October 2005/Accepted: 9 January 2006
Published online: 11 February 2006 •

ABSTRACT The momentum transfer and the specific impulse of the ablative laser propulsion of nanosecond laser irradiation on copper, lead, aluminum and graphite targets are investigated. The effects of the ambient pressure and laser focal spot sizes on the target momentum are measured. The results show that the target momentum strongly relates to the ambient pressure and target property. The highest target momentum about 2.28 g · cm/s is obtained on lead targets under 1 atmospheric pressure. With the increase of the focal spot sizes, the specific impulse decreases. The highest specific impulse in vacuum is about 950 s on copper targets.

PACS 52.75.Di; 52.38.Mf; 52.50.Jm

1 Introduction

Ablative laser propulsion (ALP) has attracted much attention due to its unique advantages such as high specific impulse and low cost in comparison with other propulsive techniques [1–3]. Since Kantrowitz first proposed laser ablation as an alternative to chemical fuels to drive space vehicles in 1972 [4], many experiments on momentum transfer have been performed with various target materials and laser systems [5–8]. Those experiments mainly focused on the measurements of target impulse generated by high power CO_2 laser pulses [9, 10]. However, the physics of the mechanisms of ALP strongly depend on the ambient pressure, pulse duration and laser intensity etc.. For example, when a high power laser pulse of microsecond duration interacts with a target in air, a laser-supported detonation (LSD) wave or a laser-supported combustion (LSC) wave is formed in front of the target. These waves are the main thrust sources [6]. However, if the ambient pressure is too low, these waves cannot be formed and the impulse is directly generated from the plasma expansion [8, 11]. In early 1974, Ready investigated the effects of the ambient pressure on the target momentum using submicrosecond CO_2 laser pulses [12]. Up until now, no experiment has used nanosecond laser pulses to investigate the characteristics of ablative laser propulsion under different ambient pressures. This paper provides the measurements of target momentum and specific impulse of ALP driven by nanosecond laser pulses under different ambient pressures. Simplified analysis are given to understand the results dependence on the experimental conditions.

✉ Fax: +86-10-82649356, E-mail: jzhang@aphy.iphy.ac.cn

2 Experiments and results

The measurement of target momentum was performed in a vacuum chamber using a simple pendulum. The schematic of the experimental setup is shown in Fig. 1. The pendulum was installed on a stage driven by a microstep motor, which controls the distance between the lens and target. The laser pulses (532 nm wavelength, 7 ns pulse duration) were focused perpendicularly on the target surface through a lens ($\Phi = 38$ mm, $F = 75$ mm)). The maximum incident laser energy on the target surface was approximately 800 mJ. The experimental parameters are summarized in Table 1. The zero position is the minimum focus point of the laser beam. And the negative positions are the positions between the focal lens and the target surface. The oscillation of the pendulum after irradiation by the drive laser pulses was recorded by a video camera through a window of the chamber. The target momentum is calculated from the oscillation amplitude and the length of the pendulum. The coupling coefficient is defined as the ratio of target momentum to the laser energy.

When a target is irradiated by a high power laser pulse in air, blow-off of the target material and breakdown of the air occur in front of the target surface. The inverse Bremstrahlung absorption of laser energy by the plasma forms an LSD wave. The plasma then expands with supersonic velocity. If the plasma density is lower than the critical density, the laser energy can be directly absorbed by the target material and the plasma expansion plays a main role in the momentum transfer. If the plasma density is higher than the critical density, the laser energy is absorbed by the LSD wave. In this case, the momentum transfer is mainly completed by the LSD wave. Figure 2 shows the dependence of target momentum on the ambient pressure at the zero target position and −1 cm target position. From Fig. 2a we can see that the target momentum increases with ambient pressure. According to Fabbro's theory [13], the laser ablation pressure on the target surface can

Target position (cm)	0	−0.2	−0.4	−0.6	−0.8	−1
Focus area (mm^2)	0.114	0.2057	0.823	1.851	3.291	5.143
Laser intensity (W/cm^2)	1.143×10^{11}	0.556×10^{11}	0.139×10^{11}	0.617×10^{10}	3.47×10^{9}	2.22×10^{9}

TABLE 1 Experimental parameters

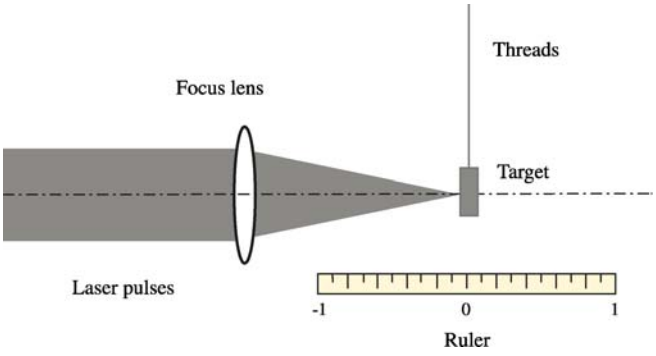

FIGURE 1 Schematic of the experimental setup

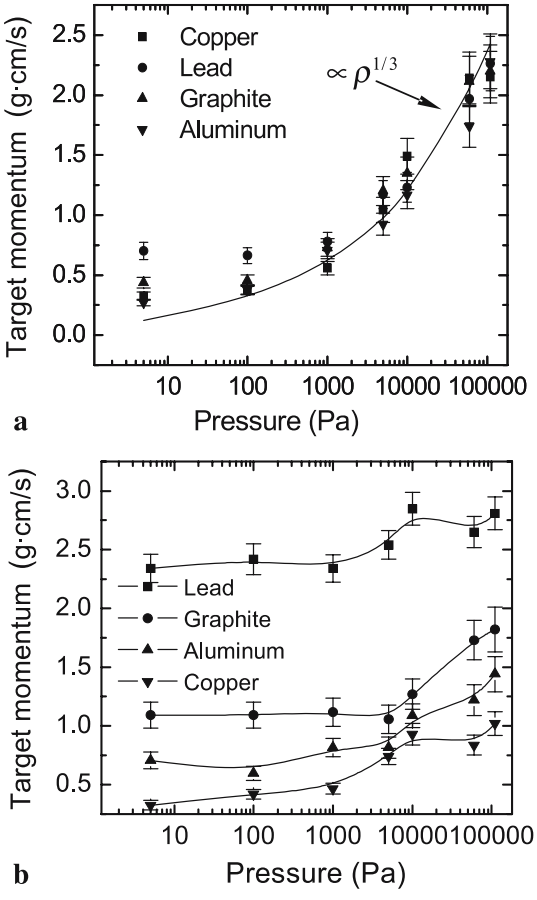

FIGURE 2 Target momentum as a function of ambient pressure (*dots*) at the zero target position (**a**) and at the −1 cm target position (**b**). The *solid line* is the theoretical approach

be written as

$$P = 32.2\left(\frac{\alpha}{2\alpha+3}\right)^{2/3}\varrho^{1/3}I^{2/3}, \tag{1}$$

where P is the pressure on the target surface, ϱ is the ambient density in front of the blast wave, α is the energy coupling coefficient and I is the laser intensity. It can be seen from this formula that the pressure on the target surface increases with the ambient density and laser intensity. The target momentum is proportional to $\varrho^{1/3}$. The experimental results at a small focal spot agree well with this analytic formula. However, for a large focal spot at −1 cm target position, the momentum transfer efficiency strongly depends on the atomic number of the target material.

The formula (1) is derived from the one-dimensional geometry and it well agrees with the experimental results at small focal spots. For a large focal spot, the target momentum should be better described by Eq. (1). However, the target momentum in Fig. 2b does not agree well with Eq. (1) but depends more on the target property. For a large focal spot, the laser intensity decreases accordingly. This results in a low intensity of the LSD wave. Under these conditions, besides the LSD wave and the laser plasma, the target momentum is also determined by target property, such as the melting temperature, and boiling temperature as well as the thermoconductivity of the target.

We can deduce from (1) that for a fixed ambient pressure and laser energy, the target momentum is proportional to $I^{-1/3}$. This means that the target momentum decreases when the target moves toward to the geometrical focal position (the minimum focus of the laser). Experimental results in Fig. 3 agree with this tendency when the target surface is located before the geometry focal position. But the target momentum presents a local maximum at the geometry focal position under 1 atmospheric pressure. This phenomenon may originate from different status of the blast wave. When the focal spot size is large, the hydrodynamics of the plasma can be described by the planar blast wave theory [14]. So target momentum firstly presents a decrease with target position. When the target closes in to the geometry focal position, the blast wave becomes a point source wave and Fabbro's theory is not suitable for this situation. In fact, at the geometry focal position, higher laser intensity can lead to an effective absorption of laser energy by the plasma. A stronger LSD wave is formed and finally results in a larger target momentum. After the geometrical focal position, the target momentum presents a rapid decrease. This attributes to the absorption of laser energy by the air plasma at the focus. But in vacuum, there is no difference in the momentum transfer for the target located behind or in front of the laser minimum focal position as shown in the curve c in Fig. 3. For other target materials, the target momentums have similar characteristics like lead targets. Comparing our results with earlier experiment with CO_2 laser pulses [12], two experiments present the same tendency of the target momentum dependence on the ambient pressure. But with the target momentum dependence on the target positions, it behaves very differently. In addition to the laser wavelength, a shorter laser pulse width and a high laser intensity in our experiments lead to this difference [15–17]. For a longer laser pulse, there is more en-

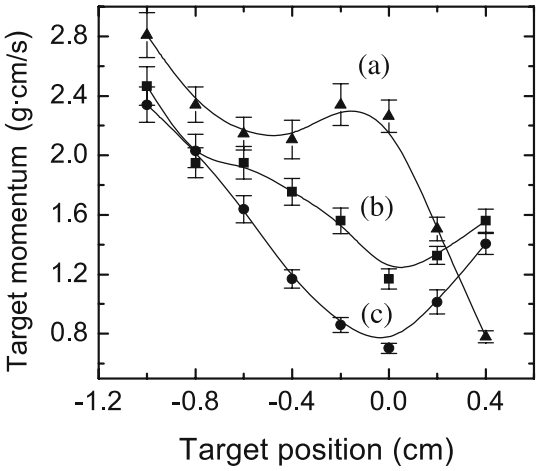

FIGURE 3 The dependence of the lead target momentum on the target positions under different ambient pressures (**a**) 1 atmospheric pressure, (**b**) 2×10^4 Pa, (**c**) 5 Pa

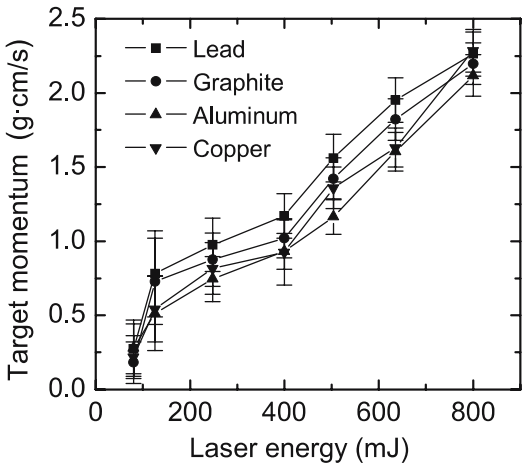

FIGURE 4 Target momentums as a function of laser energy under 1 atmospheric pressure at the geometry focal position

ergy lost in the target by thermal dissipation, and less energy converted to ablated mass. Moreover, plasma shielding and target surface reflectivity is expected to be more predominant for long pulses [17]. On the other hand, the penetration depth of laser pulses into the target material and laser generated plasma, is determined by the laser wavelength and plasma parameters. So different wavelength and widths of laser pulses lead to the difference between the experimental results. A laser beam with shorter wavelength yields a higher target momentum transfer. The effects of the higher penetration of the target surface by the longer wavelength are relatively small compared with the effects caused by the plasma absorption.

In vacuum, the target momentum is only generated by the plasma expansion from the target surface. This problem was investigated by Phipps in earlier years. According to the Phipps's formula, the ablation pressure on a target surface can be written as [7]

$$p = 5.83 A^{-1/8} \Psi^{9/16} I^{3/4} (\lambda \sqrt{\tau})^{-1/4}, \tag{2}$$

where $\Psi = A/2\left[Z^2(Z+1)\right]^{1/3}$, A is the atom mass of the target material, Z is the average charge number of ion, λ is the wavelength of the drive laser, I is the drive laser intensity and τ is the laser pulse width. It can be deduced from this formula that for a fixed drive laser energy, target momentum is proportional to $I^{-1/4}$. This can be seen from curve c in Fig. 3. We also investigated the effects of incident laser energy on the target momentum in atmospheric pressure as shown in Fig. 4. It shows that high laser energy generates a large target momentum. But the target momentum does not vary much for different target material This is due to the target momentum at a high laser intensity mainly determined by the LSD wave not the target property. The largest target momentum of a lead target is about $2.28\,\mathrm{g \cdot cm/s}$, this corresponds to a coupling coefficient of about $6.5\,\mathrm{dyne \cdot s/J}$.

Another important parameter for evaluation of the propulsion efficiency is the specific impulse, which is defined as the impulse generated by unit weight of propellant. In experiments, the specific impulse is the ratio of the target momentum to the ablation mass irradiated by a single pulse. The ablation mass is obtained by weighing the target mass before and after the laser ablation. In order to reduce the experimental error in measurement of the ablation mass, every ablation point on target surface was irradiated by one hundred shots and the total number of shots was about one thousand for a fixed target position. Figure 5 shows the specific impulse as a function of target position under vacuum. We can see from this figure that the specific impulse shows a decrease with the target approaching the geometrical focal position. This phenomenon is related to many factors. An important one is the sputtering of target material. When targets are irradiated by high power laser pulses, the surface layer is ionized into a plasma. Accompanied by the plasma, are many un-ionized particles that can be removed from the target surface with a low velocity. These particles mainly affect the ablation mass and result in a lower specific impulse. This phenomenon is serious for soft target materials ablated with high laser intensity. Furthermore, the thermal properties of target materials can also affect the specific impulse. A good thermoconductivity can lead to a heating and vaporization of target material in deep layers. This might be the reason why the higher specific impulse is always realized on the target ma-

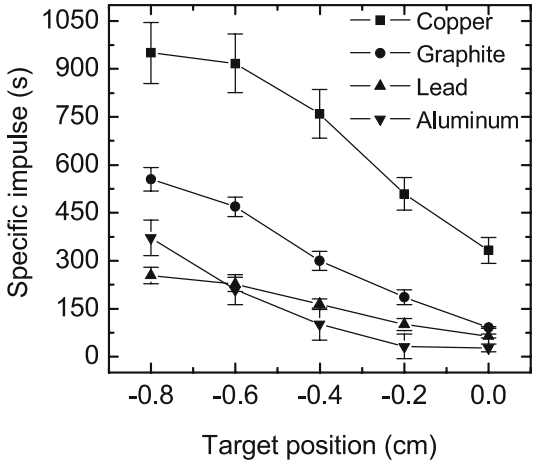

FIGURE 5 The average specific impulse as a function of target positions under 5 Pa ambient pressure

terial with a high hardness, and a high melting and boiling temperature.

3 Conclusion

In conclusion, our results show that the target momentum increases with the ambient pressure. Irradiation with a high laser intensity at the geometrical focal position, gives good experimental results which are in good agreement with the theoretical prediction. Irradiation with a low laser intensity, for a large focal spot, shows that the target momentum strongly relates to the target property. It is found that the target momentum has a local maximum at the geometrical focal position under high ambient pressure, but has a local minimum under vacuum. The highest coupling coefficient is about 6.5 dyne $\cdot$ s/J for lead target under 1 atmospheric pressure. For a fixed drive pulse energy, the average specific impulse decreases, with the target approaching the geometrical focal position. An averaged specific impulse as high as 950 s is obtained on copper targets in vacuum. But the specific impulse is strongly affected by the thermal properties of the target materials.

ACKNOWLEDGEMENTS This work was supported by the NSFC (Grant Nos. 10374116, 60128505) and National Hi-tech ICF program.

REFERENCES

1 T. Yabe, C. Phipps, M. Yamaguchi, R. Nakagawa, K. Aoki, H. Mine, Y. Ogata, C. Baasandash, M. Nakagawa, E. Fujiwara, K. Yoshida, A. Nishiguchi, Appl. Phys. Lett. **80**, 4318 (2002)
2 C.R. Phipps, M.M. Michaelis, Laser Part. Beams **12**, 23 (1994)
3 A.V. Pakhomov, D.A. Gregory, Am. Inst. Aeronaut. Astronaut. J. **38**, 725 (2000)
4 A. Kantrowitz, Astronautica Aeronautica **10**, 74 (1972)
5 S.A. Metz, Appl. Phys. Lett. **22**, 211 (1973)
6 J.E. Lowder, L.C. Pettingill, Appl. Phys. Lett. **24**, 204 (1974)
7 C.R. Phipps, T.P. Turner, R.F. Harrison, G.W. York, W.Z. Osborne, G.K. Anderson, X.F. Corlis, L.C. Haynes, H.S. Steele, K.C. Spicochi, T.R. King, J. Appl. Phys. **64**, 1083 (1988)
8 J.E. Lowder, D.E. Lencioni, T.W. Hilton, R.J. Hull, J. Appl. Phys. **44**, 2759 (1973)
9 R.L. Stegman, J.T. Schriempf, L.R. Hettche, J. Appl. Phys. **44**, 3675 (1973)
10 P.D. Gupta, P.A. Naik, H.C. Pant, J. Appl. Phys. **56**, 785 (1984)
11 S. Marcus, J.E. Lowder, J. Appl. Phys. **46**, 2293 (1975)
12 J.F. Ready, Appl. Phys. Lett. **25**, 558 (1974)
13 R. Fabbro, J. Fournier, P. Ballard, D. Devaux, J. Virmont, J. Appl. Phys. **68**, 775 (1990)
14 A.N. Pirri, R.G. Root, P.K.S. Wu, Am. Inst. Aeronaut. Astronaut. J. **16**, 1296 (1978)
15 X.L. Mao, O.V. Borisov, R.E. Russo, Spectrochem. Acta B **53**, 731 (1998)
16 X.L. Mao, A.C. Ciocan, O.V. Borisov, R.E. Russo, Appl. Surf. Sci. **127**, 262 (1998)
17 A. Bogaerts, Z.Y. Chen, Spectrochim. Acta B **57**, 1155 (2002)